

Solar Humidification Dehumidification Desalination Unit Using Trapezoidal Cross-Flow Heat Exchanger as a Dehumidifier

Ammar S. Easa¹

¹ Mechanical Department, Faculty of Technology and Education, Suez University, Suez, Egypt, email: Ammar.saad60@suezuniv.edu.eg
El-Arish High Institute for Engineering and Technology, El-Arish, North Sinai, Egypt.

DOI: 10.21608/PSERJ.2023.212263.1244

Received 21-5-2023
Revised 25-7-2023
Accepted 31-7-2023

© 2023 by Author(s) and PSERJ.

This is an open access article licensed under the terms of the Creative Commons Attribution International License (CC BY 4.0).
<http://creativecommons.org/licenses/by/4.0/>



ABSTRACT

Water is essential for life on Earth. Desalination may help alleviate the water shortage problem by transforming saltwater into drinkable water. This study examines a solar-desalination system that incorporates a humidifier and dehumidifier. This work uses a trapezoidal cross-flow heat exchanger as a dehumidifier to provide a novel method of quantifying solar humidification dehumidification (HDH) desalination. The proposed technique for dehumidification involves utilizing a trapezoidal unmixed cross-flow to enhance the condensation rate of distilled water. The number of internal trapezoidal paths, hot air flow rate, feed water flow rate, and the dehumidifier cooling technique were studied experimentally. According to the results, more internal trapezoidal paths improve productivity due to increased condensation surface area during natural cooling. Furthermore, the use of forced external cooling to increase the condensation rate is also investigated. However, the suggested system can produce about 32.6 kg of distilled water daily, and one liter of distilled water costs 0.0041\$.

Keywords: Cross-flow, Trapezoidal Heat Exchanger, Pneumatic Sprayer, Dehumidifier, Solar HDH.

1. INTRODUCTION

Desalination of saltwater and turbid water is a goal for many countries that lack adequate fresh water supplies for human usage. There is a wide variety of desalination methodologies, including solar methods [1–3], multi-stage flash methods [4–6], membrane distillation [7–9], solar still approaches [10–13], and humidification-dehumidification (HDH) methods [14–16]. HDH desalination has efficiently transformed brackish and saltwater into drinkable water at low capital and operational costs, making it a viable option for use in coastal, desert, and remote areas [17–19].

Many inventions and techniques go into the construction of HDH systems for desalination [20,21], such as water heaters [22,23], air heaters [24], humidifiers [25,26], and dehumidifiers [27,28]. Much research has been dedicated to humidifiers, and even more studies have been devoted to new and inventive humidifiers [29,30], but in practice, all researched

humidifiers will do the job. Dehumidifiers remain the primary worry restricting freshwater supplies, considering the increasing usage of humidification and dehumidification techniques.

Thermodynamics investigation of a solar HDH purification unit using fogging approach dehumidification has been examined [31]. Fresh water was pumped into the dehumidifier unit through a series of fogging nozzles to improve the condensation rate of distilled water. According to the investigation, the average production rate was around 1.70 kg per hour. However, after heating the input feedwater to 80 °C, the flow rate rose to 3.80 kg/hr. Also, investigating an HDH unit employing a closed-loop pulsating heat pipe CLPHP dehumidifier has been studied experimentally [32]. CLPHP is utilized to preheat and pre-humidify the air before entering the humidifier and exiting it from the dehumidifier. The impact of radiation and air mass flow rate on unit performance was studied. When the air mass flow was raised from 0.002 to 0.005 kg/s, the

productivity was enhanced from 0.22 to 0.52 kg/hr at 0.012 \$/L.

On the other hand, solar-powered natural vacuum desalination systems in Asia have been challenged to estimate productivity and economy via water-filling and air-releasing [33]. The system's yearly freshwater output, efficiency, and freshwater cost were analyzed for six Asian cities. Chennai had the highest annual freshwater productivity at 30.86 t/yr, Jizan had the lowest freshwater cost at 5.31 \$/t, whereas Muscat had the best thermal efficiency at 79.41% and the highest efficiency at 76.96%. Additionally, desalination systems that use ground heat exchangers to create hydrogen and potable water have been investigated [34]. The effects of solar radiation, mass flow, and soil temperature on PV-thermal panel output, efficiency, and water supply have all been analyzed. Solar radiation, soil hydrogen, fresh water, and acquired output ratios influenced system performance. The productivity ranged from 0.08 to 0.16 kg/h with a GOR of 0.1 to 0.5. The simulation of a water-cooled dehumidifier for an HDH desalination plant was considered [35]. A water-cooled condenser was employed to maximize the amount of usable freshwater produced in the smallest possible footprint. The outcome shows that using a condenser heat exchanger has 3.32 L/h of freshwater productivity.

The HDH desalination system with a dual-stage dehumidifier was tested [36]. The heat pump transfers heat from the second-stage dehumidifier to the seawater. The productivity was analyzed as a function of ocean temperature, air temperature, and airflow rate. According to the findings, the system's maximum production was 22.26 L/h at 0.051 \$/L. Furthermore, HDH thermal design was experimentally investigated. [37]. Four polypropylene plates and tubes were tested as dehumidifiers. The results indicated that a daily output of 700 liters was possible from the system.

Humidification, dehumidification, and desalination systems have also been the subject of theoretical and experimental research [38]. Fifteen different kinds of packaging were analyzed using Scilab. The results show that a high surface-to-volume ratio and a small diameter characterize the optimal packing material. Those results align with experimental testing conducted at a pall ring with a 25-millimeter-diameter metal packing.

Researching how fog affects high-drainage-area (HDH) and desalination systems [39]. The study investigated the influence of droplet dimensions on entropy generation by using a conventional jet nozzle and two fogging nozzles that generated droplets measuring 20 and 30 microns, respectively. The creation of specific entropy was reduced by a more significant margin using a 20-micron nozzle instead of a 30-micron nozzle. Maximum water output (0.85 L/h) and GOR (3.4) were accomplished at a mass flow rate ratio of 0.78. There was also an effort to optimize cycles via irreversibility analysis. It was shown that reducing the process's unique entropy production might increase the acquired output

(GOR) ratio. An alternate mechanistic model was proposed by [40]. The findings demonstrated that expanding the packing's specific area increased the recovery ratio by 16%, resulting in even more impressive freshwater water production.

Recirculation of brine in the HDH unit was examined [41]. The humidifier made use of packing fill and sprayed water. The exit temperature and feed salinity were measured. A higher salinity in the feed water was observed to result in less water being produced. Low-density (HD) hybrids (HDH) have been studied [43] for their potential to harness electricity from low-quality sources. Humidifier, dehumidifier intake air, feed temperature, and mass flow rate were analyzed for their effects on performance. The research concluded that the water productivity was around 1.398 kg/h.

This work proposed an unmixed trapezoidal cross-flow heat exchanger as a novel dehumidification technology. Therefore, this research examines the performance of a solar-HDH unit equipped with an unmixed trapezoidal cross-flow heat exchanger with a multi-trapezoidal pass in a controlled laboratory environment. Increased condensation area is achieved using a multi-trapezoidal pass dehumidifier. The dehumidifier has much surface area, allowing the humid air to condense efficiently. This study investigates the number of internal trapezoidal paths, hot air flow rate, feed water flow rate, and the dehumidifier cooling technique.

2. EXPERIMENTAL SETUP AND METHODOLOGY

The experimental apparatus utilized in the present study was employed to construct a desalination system for seawater, as illustrated in Fig. 1. A series of experiments were conducted daily in Suez, Egypt, starting at 8:00 am and ending at 5:00 pm (29.9668 °N 32.5498 °E). The current investigation comprises four fundamental elements: the humidifier, solar hot water cycle, solar hot air cycle, and dehumidifier.



Figure 1: The experimental setup as photographed.

2.1 Feed Water Cycle

The feed water cycle comprises interconnected components, including an evacuated solar collector, gate valve, water flow meter, and pipeline. Utilizing solar radiation to warm salt water within an evacuated solar collector is employed. The apparatus comprises a receiver having a volume of 200 L and 20 evacuated tubes. The tubes have a length of 2.10 m, an internal bore of 0.047 m, and an external bore of 0.058 m. In Suez, Egypt, the evacuated sun collector is tilted at an inclination of almost 25 degrees. The pipeline is constructed from polypropylene material with a melting point of 160 °C. The gate valve was employed to control the hot water flow rate.

2.2 Feed Air Cycle

Utilizing solar radiation to warm the air before its introduction into the humidifier to enhance the vaporization rate is commonly known as the solar hot air cycle. The solar air cycle comprises four fundamental components. (pipeline, dual blowers, and dual solar air heaters). The fabrication of solar air heaters involves the utilization of galvanized steel. The collector is 120 centimeters in length, 70 centimeters in breadth, 10 centimeters in height, and 0.001 millimeters in thickness. The collector is inclined at an angle of 25 degrees and features an upper glass surface with a thickness of 5 cm.

2.3 Humidification Section

The humidification section permits humidified to the desalination system. It's the central processing unit for the proposed approach. The using of a pneumatic sprayer provides considerable moisture to hot air. Fig. 2 shows the pneumatic humidifier attached to the humidification section. The humidification section, 0.60 m wide by 0.60 m high, comprises 0.001 m galvanized steel sheets. Also, the humidification front section is transparent, allowing for monitoring. The humidifier's surface was insulated with 0.05 m glass wool to reduce losses. A pneumatic sprayer humidifies by atomizing hot water with compressed air. Pressured air impinges on the water to create small hot water splashes. The pneumatic nozzle diameter was selected to be 0.0010 m.



Figure 2: Photograph of the humidification section.

2.4 Dehumidification Section

The dehumidifier consists of multi-trapezoidal channels cross flow heat exchanger to concentrate the water vapor to condensate on the heat exchanger surface. Fig. 3 shows a photograph of the dehumidification section. Humid air streams via the inner channels while the ambient air flow naturally/forced through the outside perpendicular channels. The inside channels have a trapezoidal shape to collect the distilled water at the bottom of the trapezoidal channels. The dehumidifier's physical measurements are 0.60×0.80×0.60 m, and it is fabricated using galvanized steel sheets with a thickness of 0.005 m. The trapezoidal cross-flow heat exchanger is studied with the natural ambient flow at different channel numbers. Also, it is investigated using forced air flow via an electrical fan with varying air velocities.



Figure 3: Photograph of the dehumidification section.

2.5 Measurements

The experimental setup was employed to examine various parameters to enhance the existing system's efficiency. The temperatures of the hot saline water, hot air, and humid air were considered before and after the humidification section. Further, the flow rates for air and warm seawater mass were computed. Furthermore, solar irradiance and the accessibility of potable water are documented. Table (1) presents the locations where the measurements were taken. Further, Table (2) shows a comprehensive overview of the measuring instruments and their corresponding levels of precision.

Table 1. Measurements positions in the proposed installation.

Item	Position
Radiation	Ambient
Productivity	After the dehumidifier
Water flow rate	Before the humidifier
Air velocity	Before the humidifier
Temperature	In the hot water storage tank
	Before the humidifier
	After the humidifier
	Before the solar air collectors
	After the solar air collectors
	In the humidifier shell
	Before the dehumidifier
	In the dehumidifier
	Distilled water
	On the dehumidifier's outer surface
Humidity	Before the solar air collectors
	After the solar air collectors
	In the humidifier shell
	After the dehumidifier
	Between dehumidifier and humidifier

Table 2. Measurements Specifications.

Item	Device	Model	Range	Item
Production	Graduated cylinder	Graduated cylinder	0:1000 mm	± 10 mm ³
Solar Energy	Solar Meter	TM-207	0:2kW.m ⁻²	±10 W.m ⁻²
Relative humidity	Humidity meter	Brannan	0:100 %	± 1%
Air velocity	Anemometer	GM8908	0:3 m.s ⁻¹	±0.05 m.s ⁻¹
Temperature sensor	Thermocouple	K type	-270:1372 °C	± 1%
Flow rate	Digital flow meter	FS300A	1:60L.min ⁻¹	± 3%

3. UNCERTAINTY INVESTIGATION

The standard margin of error is calculated using the following formula to evaluate the accuracy of the instruments [42]:

$$U = \frac{\alpha}{\sqrt{3}} \quad (1)$$

The letter "U" denotes the standard measurement uncertainty, while the symbol "α" represents the instrument's accuracy. Table 3 displays both scenarios' measurement range, accuracy, and expected legal uncertainty.

Table 3. The measurement system's standard uncertainties.

Measuring	Rang	Accuracy	Standard Uncertainty
Tachometer	0:9999 rpm	0.04% ± 2	0.02309
Solar Meter	0:2 kW/m ²	± 10	5.773
Humidity meter	0:100%	± 1%	0.00577
Anemometer	0:30 m/s	± 0.05	0.0288
K-type thermocouple	-270:1372 °C	± 1%	0.00577
Flow meter	1:60 L/min	± 3%	0.0173

The equations presented below can be utilized to assess the level of uncertainty linked with a given outcome [14].

$$R=f(Z_1, Z_2, Z_3, \dots, Z_n) \quad (2)$$

$$\Delta R = \sqrt{\left(\frac{\partial R}{\partial Z_1} \Delta_1\right)^2 + \left(\frac{\partial R}{\partial Z_2} \Delta_2\right)^2 + \left(\frac{\partial R}{\partial Z_3} \Delta_3\right)^2 + \dots + \dots + \left(\frac{\partial R}{\partial Z_n} \Delta_n\right)^2} \quad (3)$$

R denotes the investigational outcome, R represents the uncertainty in this outcome, and the uncertainties in the other variables, Z₁, Z₂, Z₃,.....Z_n is characterized by Δ₁, Δ₂, Δ₃ respectively. The estimated uncertainties of the experimental result indicate that the uncertainties ranged from 0.007424 to 0.210354.

4. OUTCOMES AND DISCUSSION

This present study investigates the performance of a solar HDH desalination system utilizing a trapezoidal heat exchanger as a dehumidifier. The number of internal trapezoidal paths, hot air flow rate, feed water flow rate, and the dehumidifier cooling method are all investigated.

4.1 The Influence of the Number of Internal Trapezoidal Paths on Freshwater Productivity

The cross-flow heat exchanger's internal trapezoidal paths were studied in the present work at nine values: single, double, triple, quadruple, quintuple, hexa, seven, octal, and nine paths. Fig. 4 explores the effect of the number of cross-flow heat exchanger's internal trapezoidal paths on accumulated and hourly water productivity. The productivity is influenced by solar power, with more excellent productivity rates occurring at higher solar power levels (at noon duration). Additionally, it was noted that the increased internal trapezoidal paths improved productivity on an hourly and cumulative basis.

When using a trapezoidal cross-flow heat exchanger dehumidifier with a single internal trapezoidal path, the daily accumulated productivity was about 2.5 kg/day. And the exit air relative humidity was noted to be more than 95%. That is, the dehumidification process was not carried out efficiently. Therefore, the dehumidification procedure was tested by doubling the number of internal trapezoidal paths.

When using a trapezoidal cross-flow heat exchanger dehumidifier with a double, triple, quadruple, quintuple, hexa, seven, octal, and nine internal trapezoidal paths, the daily accumulated productivity were about 4.7, 6.9, 9.2, 11.3, 13.7, 16, 18.1, and 19.9 kg/day. The enhancement was 88, 180, 270, 350, 440, 540, 620, and 690% with double, triple, quadruple, quintuple, hexa, seven, octal, and nine internal trapezoidal paths. And the exit air relative humidity was about 92, 90, 87, 85, 81, 77, 74, and 70 %. One could say that increasing the number of internal trapezoidal paths expands the condensation surface area and, as a result, enhances freshwater productivity.

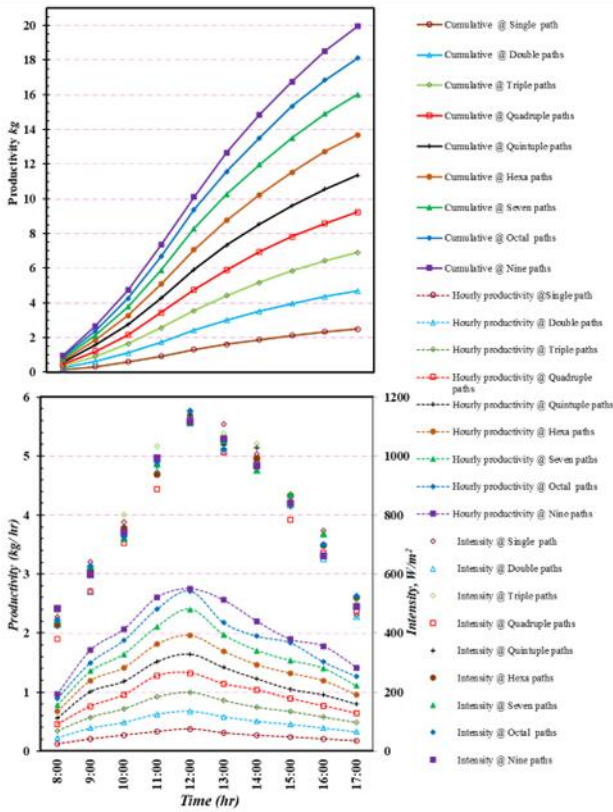


Figure 4: The effect of the number of internal trapezoidal paths on freshwater productivity.

4.2 The effect of the humid air flow rate on water production

This study intended to examine the flow rate of humid air across six different amounts, specifically 0.065, 0.082, 0.106, 0.131, 0.164, and 0.187 kg/s. The impact of different rates of humid airflow on water generation is analyzed in Figure 5. The water desalination rate depends on solar radiation, with higher levels of solar energy resulting in increased water production rates. (at noon duration). Moreover, it has been documented that an increase in the rate of humid airflow led to an elevation in both the hourly and cumulative water yield.

The results indicate that an increase in airflow rate is associated with a reduction in the output temperature of the solar air collector. At midday, an air temperature increase is observed at the flat plate solar collector outlet across all airflow rates. Furthermore, the augmentation of airflow velocity amplifies the heat transfer rate within the solar collector, resulting in a reduction of air temperature at the outlet of the solar collector. The augmentation of solar radiation at noon causes a necessary rise in the temperature of sprayed water, leading to increased heat transfer rates. This phenomenon is ascribed to a rise in entrained water vapor, which leads to a subsequent augmentation in the temperature of the air that is discharged from the humidifier. The convective air is mixed with the water

vapor produced by a pneumatic humidification system. As a result, the level of moisture rises.

A daily accumulated productivity of approximately 19.9 kg/day was observed using 0.065 kg/s of humid air through nine internal trapezoidal paths. Consequently, the efficacy of the dehumidification process was evaluated by augmenting the velocity of humid air. The daily accumulated productivity of humid air with flow rates of 0.082, 0.106, 0.131, 0.164, and 0.187 kg/s were found to be about 20.9, 21.4, 22.6, 23.5, and 24.4 kg/day, respectively. The observed enhancements were 5%, 7.5%, 13.5%, 18.3%, and 22.5% in sequence, while the corresponding flow rates were 0.082, 0.106, 0.131, 0.164, and 0.187 kg/s. Furthermore, the peak daily productivity is achieved when the airflow rate is 0.187 kg/s, accompanied by a 22.5% proportion.

4.3 Effect of feed water flowrate on production

The experimental evaluation of the proposed desalination system involved the manipulation of the feed water flow rate at six discrete levels, specifically 0.005, 0.007, 0.009, 0.011, 0.013, and 0.015 kg/s. However, the volumetric air flow rate was constant at 0.187 kilograms per second during the experimental trials. Increasing the feedwater flow rate improves the contact area between the airflow and the feedwater spraying flow, increasing the heat transfer coefficients and the mass transferred. The feedwater flow rate affects hourly and daily output differently, as shown in Figure 5. Daily accumulated productivity of approximately 24.4 kg/day was observed using 0.005 kg/s of feedwater through nine internal trapezoidal paths and 0.187 kg/s of humid air. The daily accumulated productivity of feedwater with flow rates of 0.005, 0.007, 0.009, 0.011, 0.013, and 0.015 kg/s were found to be about 25.8, 27.4, 28, 27.7, and 26.13 kg/day, respectively. The observed improvements were 5.6%, 12.2%, 14.6%, 13.4%, and 6.9%, respectively, with corresponding flow rates of 0.007, 0.009, 0.011, 0.013, and 0.015 kg/s. Furthermore, the peak daily productivity is achieved when the feedwater flow rate is 0.011 kg/s, resulting in a 14.6% output.

4.4 Influence of dehumidifier external forced convection on freshwater productivity

The free-convection trapezoidal cross-flow dehumidifier cannot effectively cool and condense the condensation surfaces when exposed to a significant amount of moisture in the air at an increased airflow rate. Therefore, there is a necessity to utilize forced air. Forced convection is a distinct mode of heat transfer that involves the imposition of fluid motion to enhance the heat transfer rate. Various methods can induce this forcing, including using a fan.

The proposed desalination system was attached with a fan to compare the result of free convection with the forced convection results. The external forced airflow

speed was tested at 5, 8, 11, 13, and 15 m/s when the air and feed water flow rates remained constant at 0.187 kg/s and 0.011 kg/s throughout the tests. An increase in the external airspeed decreases the temperature of the dehumidifier surface and enhances the condensation process. The influence of the external airspeed on the hourly and accumulated productivity is illustrated in Figure 7.

Daily accumulated productivity of approximately 28 kg/day was observed using natural air convection through external trapezoidal paths. The daily accumulated productivity of the system with air speeds of 5, 8, 11, 13, and 15 m/s was found to be about 29.9, 30.7, 31.5, 32.1, and 32.6 kg/day, respectively. The observed improvements were 6.8%, 9.7%, 12.6%, 14.8%, and 16.5%, respectively, with air speeds of 5, 8, 11, 13, and 15 m/s.

4.5 A comparative analysis of current and past outcomes

This study aims to investigate the water production process of a solar-powered desalination system employing a trapezoidal cross-flow heat exchanger dehumidifier. The investigation involves the analysis of the system's productivity under various conditions, with varying numbers of internal trapezoidal paths, hot air flow rate, feed water flow rate, and the dehumidifier cooling method.

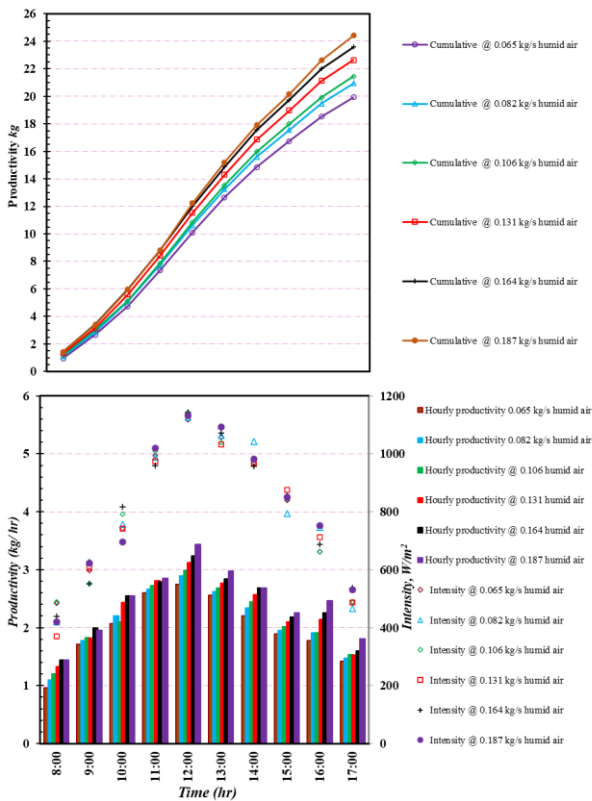


Figure 5: The impact of varying humid airflow rates on fresh water productivity.

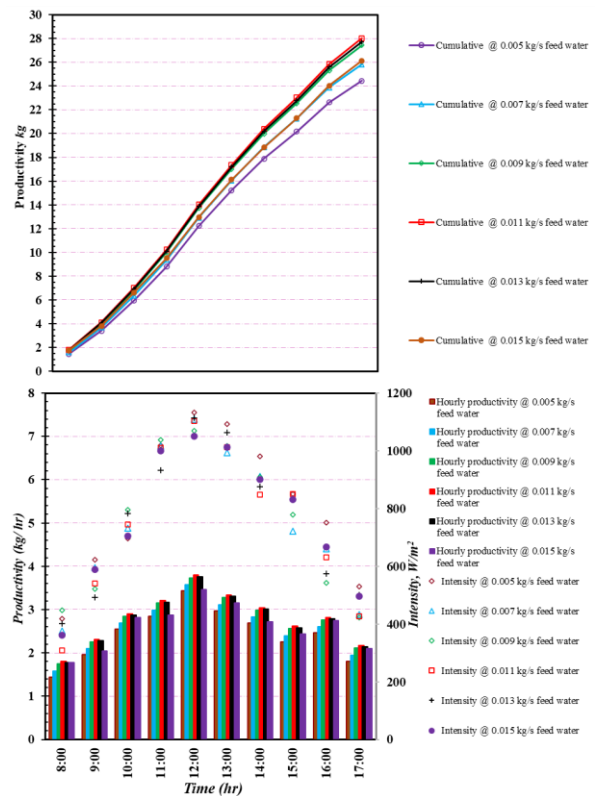


Figure 6: The impact of the feedwater flow rate on productivity at humid air flowrate of 0.187 kg/s.

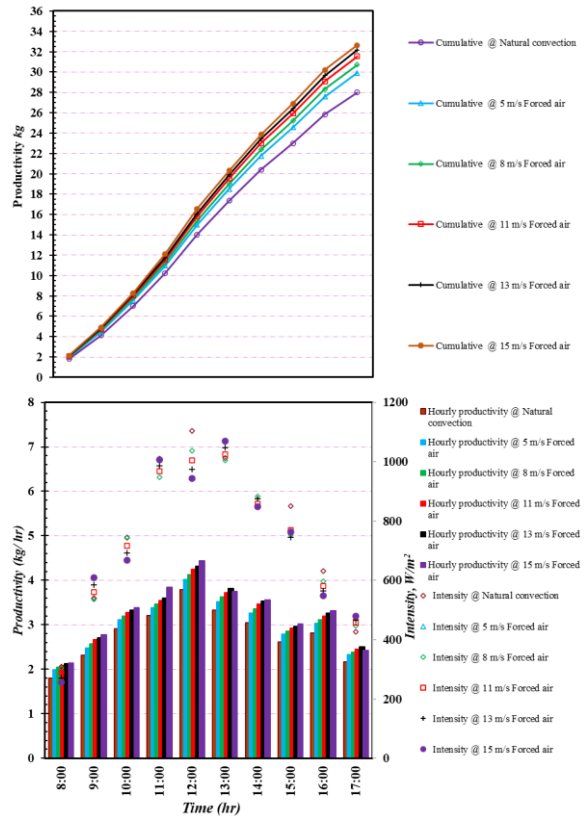


Figure 7: The influence of the external airspeed on productivity at air and feed water flow rates of 0.187 kg/s and 0.011 kg/s.

The present study compares the productivity of HDH desalination systems concerning different conditions and identifies the optimal conditions for achieving the highest productivity. The comparative analysis encompasses methodologies, output efficiency, and unit cost. The findings align with the pattern specified in the prior investigation, as indicated in Table 4. Moreover, the proposed scheme exhibits a reasonable level of freshwater productivity.

Table 4. Comparing current research to those of the past

Ref	Method	Price (\$/L)	Yield (kg)
[14]	HDH - centrifugal Sprayer	0.0106	7.9900
[25]	HDH-thermosyphon	0.0280	6.2750
[32]	HDH-heat pipe	0.0120	8.7000
[36]	HDH with heat pump	0.0510	22.260
[43]	Hybrid HDH-RO desalination system	-	192.00
[44]	Hybrid HDH system	0.0700	17.420
[45]	HDH	0.0981	5.5500
[46]	HDH -PCM	0.0110	6.5200
[47]	SS-HDH	0.0081	6.1500
Current work	HDH- natural air trapezoidal cross-flow dehumidifier	0.00475	28.10
Current work	HDH – forced air trapezoidal cross-flow dehumidifier	0.0041	32.60

5. COST INVESTIGATION

The computation of the price of distilled water is determined by sources [48,49]. Table 5 encompasses the capital expenses associated with all system equipment. The current system has an approximate retail value of 1460\$. The utilization of mass manufacturing techniques may result in a reduction of about 35% in capital costs. As a result, the costs associated with freshwater productivity are reduced. The expenses linked to installing a photovoltaic system to power the air compressor and blowers are encompassed within the scope of consideration.

Table 5. The proposed system's initial investment charge.

Element	Charge (US \$)
Photovoltaic arrangement	700
Evacuated solar collector	400
Air compressor	200
Trapezoidal Dehumidifier	60
Pneumatic nozzle	20
Blower	30
Flat plat solar collector	50
Total Charge	1460

The estimated electric power necessary to operate two blowers and an air compressor is as follows [49].

$$\text{Electric power} = \sum I \times V_{\text{air compressor}} \times \text{operating time} \times \frac{\text{Price}}{\text{kW.hr}} \quad (4)$$

$$\text{Cost / L} = \frac{\text{Capital cost} + \sum I \times V_{\text{air compressor}} \times \text{operating time} \times \frac{\text{Price}}{\text{kW.hr}}}{\text{life time} * \text{Annual total fresh water}} \quad (5)$$

$$\text{Cost / L(Using PV system)} = \frac{\text{Capital cost}}{\text{Life time} * \text{Annual total fresh water}} \quad (6)$$

Utilizing the PV system can mitigate electricity expenses and decrease the cost of freshwater productivity from 0.018382163 \$/L to 0.004084925\$/L. It could be hypothesized that this system has a lifespan of 30 years. Furthermore, the estimated cost is delineated and tabulated in Table 6 across various forced air speeds.

Table 6. The estimated cost at different forced air speeds.

Forced air speeds	Cost (\$/L) using photovoltaic	Price (\$/L) using electricity
Natural air	0.004760205	0.021420921
5 m/s Forced air	0.004455256	0.020048651
8 m/s Forced air	0.004338563	0.019523532
11 m/s Forced air	0.004225401	0.019014307
13 m/s Forced air	0.004145152	0.018653184
15 m/s Forced air	0.004084925	0.018382163

6. CONCLUSIONS

This study examines the utilization of Trapezoidal Cross-Flow Heat Exchanger Dehumidifier technology, integrated with a pneumatic sprayer-based humidifier, for solar HDH desalination systems. An experimental test rig was utilized to evaluate the performance of water production. Inferences that can be made based on the results listed above comprise:

1. One could say that the increase in the number of internal trapezoidal paths expands the condensation surface area and, as a result, enhances freshwater productivity.
2. Productivity increases by 22.5% when the feed air flow rate goes from 0.082 kg/s to 0.187 kg/s.
3. Increases in feedwater flow rate improve heat transfer coefficients by increasing the contact area between the airflow and the feedwater spraying flow. However, the peak daily freshwater productivity was recorded at 0.11 kg/s feedwater flow rate.
4. Using forced air to cool the trapezoidal cross-flow heat exchanger enhances productivity by about 16.5% at an air speed of 15 m/s.
5. The system under consideration can generate about 32.6 kilograms of distilled water daily. The unit cost of producing one liter of water is 0.0041 dollars.

7. ABBREVIATIONS

CLPHP	Closed-loop pulsating heat pipe
GOR	Gain output ratio
HDH	Humidification-dehumidification
PV	Photovoltaic
RO	Reverse Osmosis
PCM	Phase Change Material
SS	Solar Still

Declaration of competing Interest

The authors declare that they have no known competing financial interests or personal relationships that could have appeared to influence the work reported in this paper.

8. REFERENCES

- [1] A.D. Nannaware, C.M. Sai Kumar, S. Srivastava, S. Singh, M.K. Gupta, P.K. Rout, C.S. Chanotiya, R.K. Lal, Y. Nimdeo, S. Roy, Eco-friendly solar distillation apparatus for improving the yield of essential oils with enhancing organoleptic characteristics, *Renew Energy*. 191 (2022) 345–356. <https://doi.org/10.1016/J.RENENE.2022.03.147>.
- [2] G. Angappan, S. Pandiaraj, H. Panchal, T. Kathiresan, D. Ather, C. Dutta, M.K. Subramaniam, S. Muthusamy, A.E. Kabeel, A.S. El-Shafay, K.K. Sadasivuni, An extensive review of performance enhancement techniques for pyramid solar still for solar thermal applications, *Desalination*. 532 (2022) 115692. <https://doi.org/10.1016/J.DESAL.2022.115692>.
- [3] H. Fayaz, S. Rasachak, M. Shakeel Ahmad, L. Kumar, B. Zhang, JeyrajSelvaraj, M.A. Mujtaba, M. Elahi M. Soudagar, R. Kumar, M. Rasoul Omidvar, Improved surface temperature of absorber plate using metallic titanium particles for solar still application, *Sustainable Energy Technologies and Assessments*. 52 (2022) 102092. <https://doi.org/10.1016/J.SETA.2022.102092>.
- [4] M. Tayefeh, Exergy and economic analysis of a novel integration of compressed air energy storage with multi-effect distillation and multi-stage flash systems, *J Energy Storage*. 55 (2022) 105534. <https://doi.org/10.1016/J.EST.2022.105534>.
- [5] M. Tayefeh, An innovative rearrangement and comprehensive comparison of the combination of compressed air energy storage (CAES) with multi stage flash (MSF) desalination and multi effect distillation (MED) systems, *J Energy Storage*. 52 (2022) 105025. <https://doi.org/10.1016/J.EST.2022.105025>.
- [6] M. Tayefeh, Exergy and economic analysis of a novel integration of compressed air energy storage with multi-effect distillation and multi-stage flash systems, *J Energy Storage*. 55 (2022) 105534. <https://doi.org/10.1016/J.EST.2022.105534>.
- [7] J. Choi, J. Cho, J. Shin, H. Cha, J. Jung, K.G. Song, Performance and economic analysis of a solar membrane distillation pilot plant under various operating conditions, *Energy Convers Manag.* 268 (2022) 115991. <https://doi.org/10.1016/J.ENCONMAN.2022.115991>.
- [8] J. Choi, J. Cho, J. Shin, H. Cha, J. Jung, K.G. Song, Performance and economic analysis of a solar membrane distillation pilot plant under various operating conditions, *Energy Convers Manag.* 268 (2022) 115991. <https://doi.org/10.1016/J.ENCONMAN.2022.115991>.
- [9] A. Yadav, P.K. Labhasetwar, V.K. Shahi, Membrane distillation crystallization technology for zero liquid discharge and resource recovery: Opportunities, challenges and futuristic perspectives, *Science of The Total Environment*. 806 (2022) 150692. <https://doi.org/10.1016/J.SCITOTENV.2021.150692>.
- [10] A.A.V. Lisboa, R. Segurado, M.A.A. Mendes, Solar still performance for small-scale and low-cost seawater desalination: Model-based analysis and water yield enhancement techniques, *Solar Energy*. 238 (2022) 341–362. <https://doi.org/10.1016/J.SOLENER.2022.04.007>.
- [11] A.S. Abdullah, Z.M. Omara, F.A. Essa, U.F. Alqsair, M. Aljaghtham, I.B. Mansir, S. Shanmugan, W.H. Alawee, Enhancing trays solar still performance using wick finned absorber, nano-enhanced PCM, *Alexandria Engineering Journal*. 61 (2022) 12417–12430. <https://doi.org/10.1016/J.AEJ.2022.06.033>.
- [12] S.A. Mohamed, H. Hassan, Investigation the performance of new designed solar still of rhombus shaped based on new model, *Solar Energy*. 231 (2022) 88–103. <https://doi.org/10.1016/J.SOLENER.2021.11.039>.
- [13] S. Shoeibi, M. Saemian, H. Kargarsharifabad, S. Hosseinzade, N. Rahbar, M. Khiadani, M.M. Rashidi, A review on evaporation improvement of solar still desalination using porous material, *International Communications in Heat and Mass Transfer*. 138 (2022) 106387. <https://doi.org/10.1016/J.ICHEATMASSTRANSFER.2022.106387>.
- [14] R.A. Khalaf-Allah, G.B. Abdelaziz, M.G. Kandel, A.S. Easa, Development of a centrifugal sprayer-based solar HDH desalination unit with a variety of sprinkler rotational speeds and droplet slot distributions, *Renew Energy*. 190 (2022)

- 1041–1054.
<https://doi.org/10.1016/J.RENENE.2022.04.019>.
- [15] A.S.A. Mohamed, A.G. Shahdy, M. Salem Ahmed, Investigation on solar humidification dehumidification water desalination system using a closed-air cycle, *Appl Therm Eng.* 188 (2021).
<https://doi.org/10.1016/j.applthermaleng.2021.116621>.
- [16] M. Faegh, M.B. Shafii, Thermal performance assessment of an evaporative condenser-based combined heat pump and humidification-dehumidification desalination system, *Desalination.* 496 (2020).
<https://doi.org/10.1016/j.desal.2020.114733>.
- [17] A.E. Kabeel, M.R. Diab, M.A. Elazab, E.M.S. El-Said, Solar powered hybrid desalination system using a novel evaporative humidification tower: Experimental investigation, *Solar Energy Materials and Solar Cells.* 248 (2022) 112012.
<https://doi.org/10.1016/J.SOLMAT.2022.112012>.
- [18] H. Xu, X. Gu, T. Jia, Y. Dai, Experimental investigation and optimization of a solar desalination unit with high heat recovery ratio using weak air compression process, *Energy Convers Manag.* 255 (2022) 115369.
<https://doi.org/10.1016/J.ENCONMAN.2022.115369>.
- [19] B. Anand, S. Murugavelh, R. Shankar, P. Phelan, Experimental investigation on a cooling cum desalination system using a modified mechanical heat pump, *International Journal of Refrigeration.* 143 (2022) 138–147.
<https://doi.org/10.1016/J.IJREFRIG.2022.06.025>.
- [20] A.S.A. Mohamed, M.S. Ahmed, H.M. Maghrabie, A.G. Shahdy, Desalination process using humidification–dehumidification technique: A detailed review, *Int J Energy Res.* 45 (2021) 3698–3749.
<https://doi.org/10.1002/ER.6111>.
- [21] J.S. Shaikh, S. Ismail, A review on recent technological advancements in humidification dehumidification (HDH) desalination, *J Environ Chem Eng.* 10 (2022) 108890.
<https://doi.org/10.1016/J.JECE.2022.108890>.
- [22] S.W. Sharshir, G. Peng, N. Yang, M.A. Eltawil, M.K.A. Ali, A.E. Kabeel, A hybrid desalination system using humidification-dehumidification and solar stills integrated with evacuated solar water heater, *Energy Convers Manag.* 124 (2016) 287–296.
<https://doi.org/10.1016/J.ENCONMAN.2016.07.028>.
- [23] S.W. Sharshir, G. Peng, N. Yang, M.O.A. El-Samadony, A.E. Kabeel, A continuous desalination system using humidification - Dehumidification and a solar still with an evacuated solar water heater, *Appl Therm Eng.* 104 (2016) 734–742.
<https://doi.org/10.1016/j.applthermaleng.2016.05.120>.
- [24] X. Li, G. Yuan, Z. Wang, H. Li, Z. Xu, Experimental study on a humidification and dehumidification desalination system of solar air heater with evacuated tubes, *Desalination.* 351 (2014) 1–8.
<https://doi.org/10.1016/j.desal.2014.07.008>.
- [25] P. Behnam, M.B. Shafii, Examination of a solar desalination system equipped with an air bubble column humidifier, evacuated tube collectors and thermosyphon heat pipes, *Desalination.* 397 (2016) 30–37.
<https://doi.org/10.1016/J.DESAL.2016.06.016>.
- [26] P. Ranjitha Raj, J.S. Jayakumar, Performance analysis of humidifier packing for humidification dehumidification desalination system, *Thermal Science and Engineering Progress.* 27 (2022) 101118.
<https://doi.org/10.1016/J.TSEP.2021.101118>.
- [27] K. Garg, S.K. Das, H. Tyagi, Thermal design of a humidification-dehumidification desalination cycle consisting of packed-bed humidifier and finned-tube dehumidifier, *Int J Heat Mass Transf.* 183 (2022) 122153.
<https://doi.org/10.1016/J.IJHEATMASSTRANSFER.2021.122153>.
- [28] L. Zhang, K. Feng, Z. Xie, K. Wang, Study on Heat Transfer Process and Fresh Water Output Performance of Phase Change Heat Storage Dehumidifier, *Energies (Basel).* 15 (2022).
<https://doi.org/10.3390/en15041504>.
- [29] P. Ranjitha Raj, J.S. Jayakumar, Performance analysis of humidifier packing for humidification dehumidification desalination system, *Thermal Science and Engineering Progress.* 27 (2022) 101118.
<https://doi.org/10.1016/J.TSEP.2021.101118>.
- [30] S. Hussain Soomro, R. Santosh, C.U. Bak, C.H. Yoo, W.S. Kim, Y.D. Kim, Effect of humidifier characteristics on performance of a small-scale humidification-dehumidification desalination system, *Appl Therm Eng.* 210 (2022) 118400.
<https://doi.org/10.1016/J.APPLTHERMALENG.2022.118400>.
- [31] M. Alrbai, H.S. Hayajneh, S. Al-Dahidi, A. Alahmer, Thermodynamics analysis of a lab scale humidification-dehumidification desalination system employing solar energy and fogging approach, *Solar Energy.* 247 (2022) 397–407.
<https://doi.org/10.1016/j.solener.2022.10.048>.
- [32] L. Aref, R. Fallahzadeh, V. Madadi Avargani, An experimental investigation on a portable bubble basin humidification/dehumidification

- desalination unit utilizing a closed-loop pulsating heat pipe, *Energy Convers Manag.* 228 (2021) 113694. <https://doi.org/10.1016/J.ENCONMAN.2020.113694>.
- [33] M. Wei, C. Zhong, J. Liu, H. Xu, J. Chen, J. Xiang, K. Wang, H. Zheng, Productivity and economy prediction for a solar-powered natural vacuum desalination system via water-filling and air-releasing in Asia, *Energy Convers Manag.* 260 (2022). <https://doi.org/10.1016/j.enconman.2022.115570>.
- [34] E. Hürdoğan, O. Kara, Performance assessment of a desalination system integrated with ground heat exchanger for hydrogen and fresh water production, *Environ Prog Sustain Energy.* 41 (2022). <https://doi.org/10.1002/ep.13745>.
- [35] V.B. Shaik, S. Tangellapalli, Design and simulation of water-cooled dehumidifier for HDH desalination plant, *Heat Transfer.* 51 (2022) 5532–5551. <https://doi.org/10.1002/htj.22558>.
- [36] Y. Zhang, C. Zhu, H. Zhang, W. Zheng, S. You, Y. Zhen, Experimental study of a humidification-dehumidification desalination system with heat pump unit, *Desalination.* 442 (2018) 108–117. <https://doi.org/10.1016/J.DESAL.2018.05.020>.
- [37] G. Prakash Narayan, M.G. st. John, S.M. Zubair, J.H. Lienhard, Thermal design of the humidification dehumidification desalination system: An experimental investigation, *Int J Heat Mass Transf.* 58 (2013) 740–748. <https://doi.org/10.1016/J.IJHEATMASSTRANSFER.2012.11.035>.
- [38] P. Ranjitha Raj, J.S. Jayakumar, Performance analysis of humidifier packing for humidification dehumidification desalination system, *Thermal Science and Engineering Progress.* 27 (2022) 101118. <https://doi.org/10.1016/J.TSEP.2021.101118>.
- [39] M. Alrbai, J. Enizat, H. Hayajneh, B. Qawasmeh, S. Al-Dahidi, Energy and exergy analysis of a novel humidification-dehumidification desalination system with fogging technique, *Desalination.* 522 (2022) 115421. <https://doi.org/10.1016/J.DESAL.2021.115421>.
- [40] D. Kaunga, R. Patel, I.M. Mujtaba, Humidification-dehumidification desalination process: Performance evaluation and improvement through experimental and numerical methods, *Thermal Science and Engineering Progress.* 27 (2022) 101159. <https://doi.org/10.1016/J.TSEP.2021.101159>.
- [41] S. Dehghani, A. Date, A. Akbarzadeh, An experimental study of brine recirculation in humidification-dehumidification desalination of seawater, *Case Studies in Thermal Engineering.* 14 (2019). <https://doi.org/10.1016/j.csite.2019.100463>.
- [42] A.S.A. Mohamed, M.S. Ahmed, A.G. Shahdy, Theoretical and experimental study of a seawater desalination system based on humidification-dehumidification technique, *Renew Energy.* 152 (2020) 823–834. <https://doi.org/10.1016/J.RENENE.2020.01.116>.
- [43] M. Abdelgaied, A.E. Kabeel, A.W. Kandeal, H.F. Abosheisha, S.M. Shalaby, M.H. Hamed, N. Yang, S.W. Sharshir, Performance assessment of solar PV-driven hybrid HDH-RO desalination system integrated with energy recovery units and solar collectors: Theoretical approach, *Energy Convers Manag.* 239 (2021) 114215. <https://doi.org/10.1016/J.ENCONMAN.2021.114215>.
- [44] S.A. Nada, A. Fouda, M.A. Mahmoud, H.F. Elattar, Experimental investigation of air-conditioning and HDH desalination hybrid system using new packing pad humidifier and strips-finned helical coil, *Appl Therm Eng.* 185 (2021) 116433. <https://doi.org/10.1016/J.APPLTHERMALENG.2020.116433>.
- [45] E. Deniz, S. Çınar, Energy, exergy, economic and environmental (4E) analysis of a solar desalination system with humidification-dehumidification, *Energy Convers Manag.* 126 (2016) 12–19. <https://doi.org/10.1016/j.enconman.2016.07.064>.
- [46] A.W. Kandeal, N.M. El-Shafai, M.R. Abdo, A.K. Thakur, I.M. El-Mehasseb, I. Maher, M. Rashad, A.E. Kabeel, N. Yang, S.W. Sharshir, Improved thermo-economic performance of solar desalination via copper chips, nanofluid, and nano-based phase change material, *Solar Energy.* 224 (2021) 1313–1325. <https://doi.org/10.1016/J.SOLENER.2021.06.085>.
- [47] A.E. Kabeel, E.M.S. El-Said, Experimental study on a modified solar power driven hybrid desalination system, *Desalination.* 443 (2018) 1–10. <https://doi.org/10.1016/j.desal.2018.05.017>.
- [48] M.I. Zubair, F.A. Al-Sulaiman, M.A. Antar, S.A. Al-Dini, N.I. Ibrahim, Performance and cost assessment of solar driven humidification dehumidification desalination system, *Energy Convers Manag.* 132 (2017) 28–39. <https://doi.org/10.1016/J.ENCONMAN.2016.10.005>.
- [49] A.S. Easa, S.M. Mohamed, W.S. Barakat, M.I.A. Habba, M.G. Kandel, R.A. Khalaf-Allah, Water production from a solar desalination system utilizing a high-speed rotary humidifier, *Appl Therm Eng.* 224 (2023) 120150.